

Supporting Information

Improving analyte selectivity by post-assembly modification of metal-organic framework based photonic crystal sensors

A. von Mankowski,^a K. Szendrei-Temesi,^a C. Koschnick^a, and B. V. Lotsch^a

^a Max Planck Institute for Solid State Research, Heisenbergstr. 1, 70569 Stuttgart, Germany

Department of Chemistry, University of Munich (LMU), Butenandtstr. 5-13, 81377 Munich, Germany

This supplementary information includes:

1. Experimental Section
2. Characterization Section
3. Supplementary Figures and Tables
4. Supplemental References

1. Experimental Section

Synthesis of CAU-1 nanoparticles: In a typical synthesis, 377 mg $\text{AlCl}_3 \cdot 6 \text{H}_2\text{O}$ (1.55 mmol) and 93.3 mg 2-aminoterephthalic acid (0.515 mmol) were dissolved in 10 mL methanol. The solutions were heated in a microwave (Biotage Initiator, Biotage) at 140 °C for 2 min. The product was obtained by centrifugation at 24 krpm for 10 min and washed twice with 20 mL methanol. The particles were resuspended in methanol by ultra-sonication. To remove agglomerates, the suspension was centrifuged at 9 krpm and filtered with a 0.45 μm PTFE filter (VWR). For spin-coating experiments, the suspension was diluted to 4 wt% with methanol.

Post-synthetic modification of CAU-1 nanoparticles: Three batches of CAU-1 nanoparticles for each modification were prepared according to the synthesis described above and merged.

For de-methoxylation of the SBU, the particles were obtained by centrifugation and heated at 200 °C for 24 h (CAU-1-SBU).

For the covalent modification, the suspended particles were washed twice with 20 mL methanol and twice with 20 mL DMF before resuspending them in 2.5 mL DMF. Then, 2.5 mL of hexanoic anhydride were added to the CAU-1 particles and heated to 80 °C for 16 h (CAU-1-Hex). The modified particles were washed twice with 20 mL MeOH. The particles were centrifuged and left to dry overnight (CAU-1-Hex).

Synthesis of TiO_2 nanoparticles: 20 mL of titanium isopropoxide were added dropwise to 36 mL of deionized water under vigorous stirring. The solution was stirred for 1 h. The resulting white solid was filtered and washed with deionized water. The remaining solid was mixed with 3.9 mL of 0.6 M tetramethylammonium hydroxide and transferred to a teflon reactor. The mixture was heated in a furnace at 120 °C for 3 h. Larger particles and agglomerates were removed by centrifugation at 13 krpm. For spin-coating experiments, the TiO_2 suspension was diluted to 3 wt% in MeOH.

Spin-coating of CAU-1/ TiO_2 Bragg stacks: Bragg stacks were produced by spin-coating the CAU-1 suspension at 6 krpm and the TiO_2 suspension at 8 krpm with a heating step at 120 °C for 5 min on 1 cm^2 silicon wafers. Three bilayers were applied (BS).

Post-assembly modification of the Bragg stacks: For post-assembly modification, the Bragg stacks were either immersed in 4 mL hexanoic acid for 16 h at 80 °C (CAU-1-Hex) or heated at 190 °C for 24 h (CAU-1-SBU). The Bragg stacks were then washed by immersion in methanol twice for at least 1 h.

Optical measurements: Prior to the measurements, the BSs were heated at 120 °C for at least 1 h in vacuo to remove residual solvents in the pores and for another 30 min in a stream of nitrogen. In order to investigate the optical response of the Bragg stacks, nitrogen gas was

bubbled through three gas washing bottles filled with the solvent to be investigated at 1.2 bar. In total, five solvents (water, methanol, ethanol, iso-propanol and heptane) were investigated. The saturated vapor stream was then introduced into a custom-built steel sample chamber with a quartz window in which the samples were fixed. Measurements were repeated at least 3 times to ensure reproducibility. To prevent errors arising from different measurement spots the sample chamber was fixed and not moved during and in between the measurements. Solvent vapor exposure was performed until the change of the reflectance was below 0.5% for a 60 seconds. After solvent vapor exposure, the chamber was flushed with pure nitrogen. To facilitate desorption of the solvent, the chamber was flushed by an alternating flow of nitrogen and saturated water vapor stream to ensure equal conditions between every measurement.

2. Characterization

Particle size distributions were determined by dynamic light scattering, DLS (Malvern Zetasizer Nano ZS, Malvern).

X-ray diffraction (XRD) patterns of powder materials were measured on a Stoe Stadi P diffractometer with Ge filtered CuK α -radiation on a DECTRIS Mythen 1K Detector (Stoe).

IR spectra were recorded on a Spectrum BX FT-IR (Perkin Elmer).

¹³C- and ¹⁵N- cross-polarization solid-state NMR (CP-ssNMR) measurements were performed on a Bruker Avance III HD 500 MHz (500 MHz, 11.74 T, Bruker) under magic angle spinning at 10 kHz using a ramped-amplitude (RAMP) CP pulse on ¹H, centered on the $n = +1$ Hartmann-Hahn condition. Contact times in ¹³C- ssNMR were 4 ms for all samples, whereas in ¹⁵N-ssNMR, contact times were 5 ms for all samples. The ¹³C and ¹⁵N chemical shifts were referenced relative to TMS and nitromethane, respectively. For ¹H liquid NMR, samples were digested in NaOD/D₂O and measured on a Bruker AV400TR NMR (400 MHz, 9.39 T, Bruker) spectrometer.

Cross-sectional SEM images were acquired on a Zeiss Merlin (Carl Zeiss AG) at acceleration voltages of 1.5 kV.

Elemental analysis was performed on a Vario micro (Elementar Analysensysteme GmbH).

Grazing-incident wide-angle X-ray scattering (GIWAXS) X-ray scattering experiments were performed using an Anton Paar SAXSpace at the LMU Munich, working group of Thomas Bein. A Xenocs GeniX3D microfocus X-ray source was used with a Cu target to generate a monochromatic beam with a 0.154 nm wavelength. A Dectris EIGER R 1M detector was used to collect the 2D scattering patterns. The GISAXS experiments were conducted with an incident angle near 0.23°. A sample-to-detector distance of 200 mm was used.

Ad- and desorption isotherms were measured on an Autosorb iQ-MP2 (Quantachrome Instruments) with argon of 99.9999% purity at 87 K and water (Milli-Q® Millipore) at 15 °C. Prior to the measurements, the samples were outgassed under high vacuum at 120 °C for at least 12 h. In accordance with the ISO recommendations, multipoint BET tags equal or below the maximum in $V \cdot (1 - p/p_0)$ were chosen. Correlation coefficients of all calculated BET surface areas were above 0.9999. For DFT pore size distribution calculations the calculation model "Ar at 87K zeolites/silica (spher./cylindr. pores, NLDFT equ.)" was used. Contact angle measurements were performed with MilliQ water on an Attension Theta Lite (Biolin Scientific).

Ellipsometric porosimetry measurements were carried out on a PS-1000 (Semilab) at an incident angle of 60.25° in the spectral range of 186.23 to 987.24 nm. For data evaluation the model and fitting range was limited from 300 to 1000 nm using a Cauchy-Lorentz model. Measurements were carried out on thin films of CAU-1, CAU-1-SBU and CAU-1-Hex. Thin films of CAU-1-SBU and CAU-1-Hex were obtained by applying the same modification procedure as for the BSs.

For time-dependent reflectance measurements a fiber optic spectrometer USB4000-XR1-ES (Ocean Optics) integrated with an optical light microscope DM2500 M (Leica) was used. The reflectance intensities were monitored at several wavelengths. The spectral shifts were calculated out of the Bragg peaks as $\Delta \lambda = \lambda_{\text{solvent}} - \lambda_{\text{N}_2}$.

Color image analysis by principal component analysis (PCA) was performed according to procedure described previously.^[1] Briefly, images of the BS were acquired during nitrogen exposure and during analyte exposure upon saturation. The images were aligned, an area selected, cropped and splitted into RGB channels. The mean intensities of the R, G and B channels were then used for PCA using the program Origin 2017 (OriginLab Corporation, USA). The combined array was calculated based on the differences in the RGB values of all three BSs.

3. Supplementary Figures and Tables

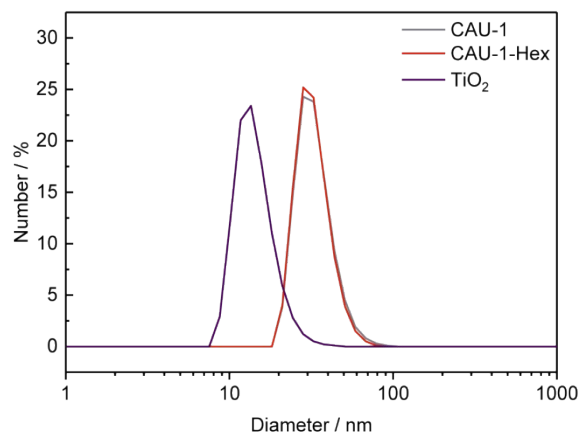


Figure S1: Size distribution of CAU-1 (0.043, grey), CAU-1-Hex (0.061, red) and TiO₂ (0.176, violet) as measured by dynamic light scattering (DLS). Polydispersity indices are given in the brackets. Note that in CAU-1 the demethoxylation of the SBUs is only possible on the dried sample.

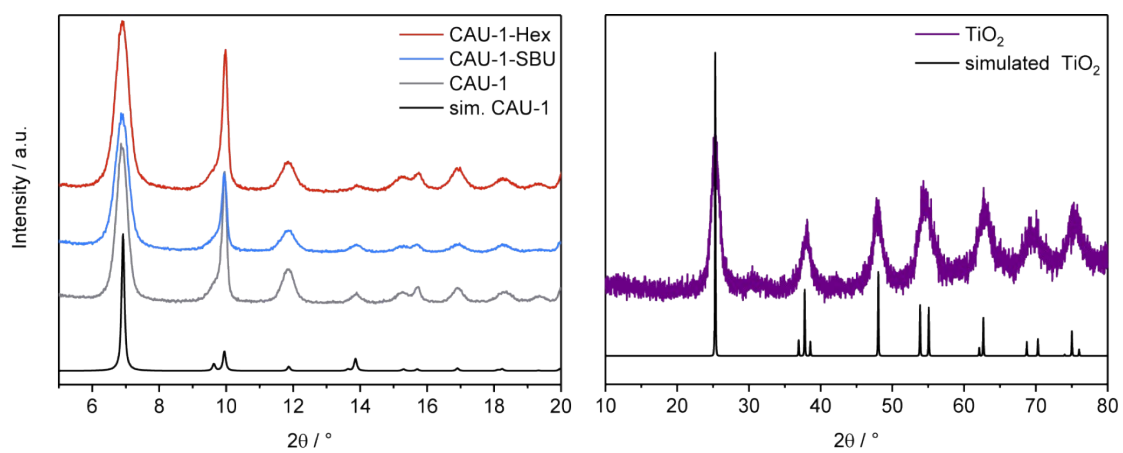


Figure S2: Powder X-ray diffractograms of (left) simulated CAU-1 (black), as-synthesized CAU-1 (grey), CAU-1-SBU (blue) and CAU-1-Hex (red), and (right) simulated TiO₂ (anatase, black) and as-synthesized TiO₂ (violet).

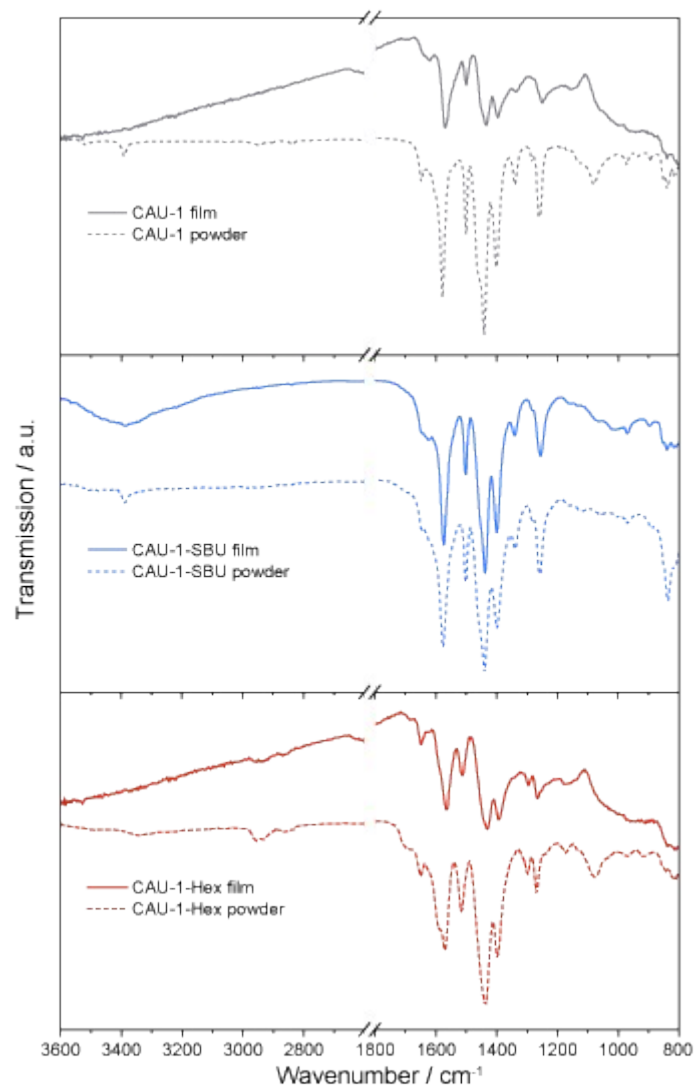


Figure S3: IR spectra of thin films of CAU-1 (grey), CAU-1-SBU (blue) and CAU-1-Hex (red) layers, dashed lines represent the powdered samples for comparison. Note that for the CAU-1-SBU films, various MOF layers were deposited to improve the signal to noise ratio.

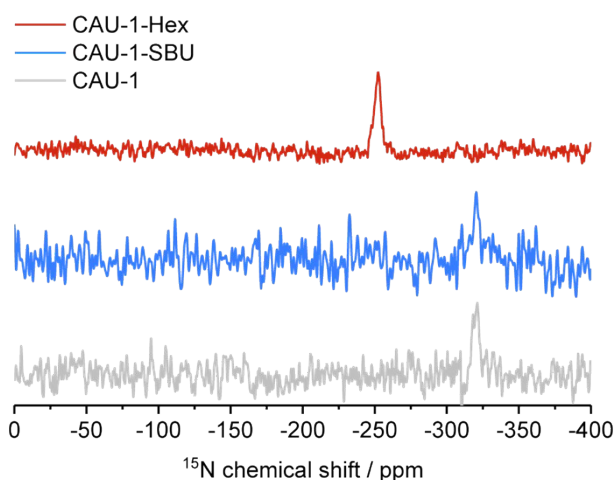


Figure S4: ^{15}N -CP-ssNMR of CAU-1 (grey), CAU-1-SBU (blue) and CAU-1-Hex (red).

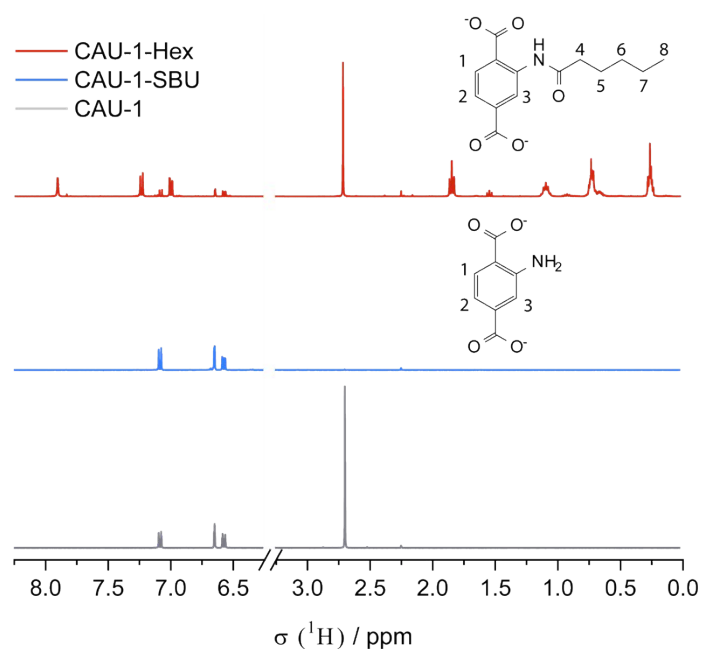


Figure S5: ^1H -NMR spectra of the directly dissolved CAU-1 (grey), CAU-1-SBU (blue) and CAU-1-Hex (red) powders. Each spectrum is normalized to the sum of aromatic H signals (methylated and unmethylated). All samples were referenced to the ^1H signal of 2H of the unmodified linker.^[2] Labelling of the ^1H signals: BDC- NH_2 : 7.07 (d, 1H, H1, $J = 8.1$ Hz); 6.64 (s, 1H, H3); 6.56 (d, 1H, H2, $J = 8.1$ Hz); BDC- $\text{NHCOCH}_2\text{CH}_2\text{CH}_2\text{CH}_3$: 7.90 (s, 1H, H3); 7.23 (d, 1H, H1, $J = 8.1$ Hz); 6.99 (m, 1H, H2); 1.85 (t, 2H, H4, $J = 7.4$ Hz); 1.09 (m, 2H, H5) 0.73 (m, 4H, H6-7); 0.25 (m, 3H, H8).

To calculate the degree of methoxylation, the integral ratios of the methoxy H-atoms: aromatic H-atoms were determined to be 1.13 for CAU-1, 0.01 for CAU-1-SBU and 1.09 for CAU-1-Hex (1:33 calc.), yielding a methoxylation degree of 85%, 1% and 82%, respectively. For CAU-1 and CAU-1-Hex the obtained degrees are in accordance with those reported in the literature.^[2] The degree of amidification was determined by the ratio of the aromatic H-atoms of the modified linker (1.00) to the total amount of aromatic H-atoms (1.19) yielding a modification degree of 84%. All samples show 1% methylation of the amine similar to those reported in the literature.^[2]

Table S1 Elemental analysis of the nanoparticle powders CAU-1-SBU, CAU-1 and CAU-1-Hex with the corresponding experimental formula and composition based on the carbon to nitrogen ratio. Crystal water and absorbed carbon dioxide are neglected.

	CAU-1-SBU	CAU-1	CAU-1-Hex
Theoretical formula	$[\text{Al}_4(\text{OH})_6-(\text{H}_2\text{N}-\text{C}_6\text{H}_3(\text{COO})_2)_3]$	$[\text{Al}_4(\text{OH})_2-(\text{OCH}_3)_4(\text{H}_2\text{N}-\text{C}_6\text{H}_3(\text{COO})_2)_3]$	$[\text{Al}_4(\text{OH})_2-(\text{OCH}_3)_4(\text{C}_5\text{H}_{11}\text{CONH}-\text{C}_6\text{H}_3(\text{COO})_2)_3]$
Theoretical composition	$\text{Al}_4\text{C}_{24}\text{H}_{21}\text{N}_3\text{O}_{18}$	$\text{Al}_4\text{C}_{28}\text{H}_{29}\text{N}_3\text{O}_{18}$	$\text{Al}_4\text{C}_{46}\text{H}_{59}\text{N}_3\text{O}_{21}$
Weight % C:N:H	29.98 : 4.33 : 4.37	38.64 : 4.97 : 3.78	47.09 : 3.75 : 5.37
Molar Ratio C:N:H	24.22 : 3.00 : 42.08	27.20 : 3.00 : 31.71	43.93 : 3 : 59.70
Experimental composition	$\text{Al}_4\text{C}_{24.22}\text{H}_{21.44}\text{N}_3\text{O}_{18}$	$\text{Al}_4\text{C}_{27.2}\text{H}_{27.4}\text{N}_3\text{O}_{18}$	$\text{Al}_4\text{C}_{43.93}\text{H}_{59}\text{N}_3\text{O}_{21}$
Degree of modification EA	96.3%	-	88.5%

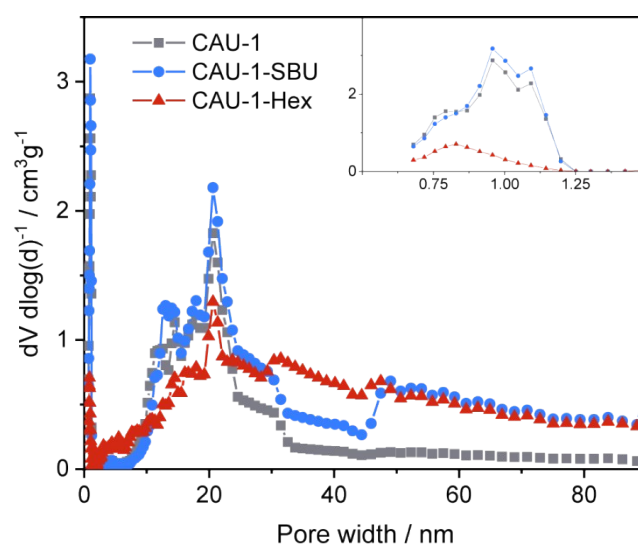


Figure S6: Pore size distributions of CAU-1 (grey), CAU-1-SBU (blue) and CAU-1-Hex (red). Fitting errors were 0.335%, 0.382% and 0.423%. Calculation details are given in Section 1.

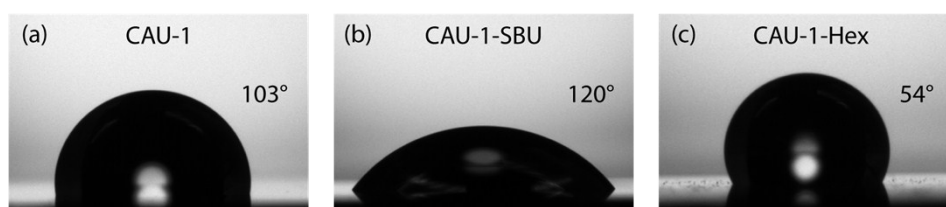


Figure S7: Contact angle measurements of different (a) CAU-1, (b) CAU-1-SBU and (c) CAU-1-Hex.

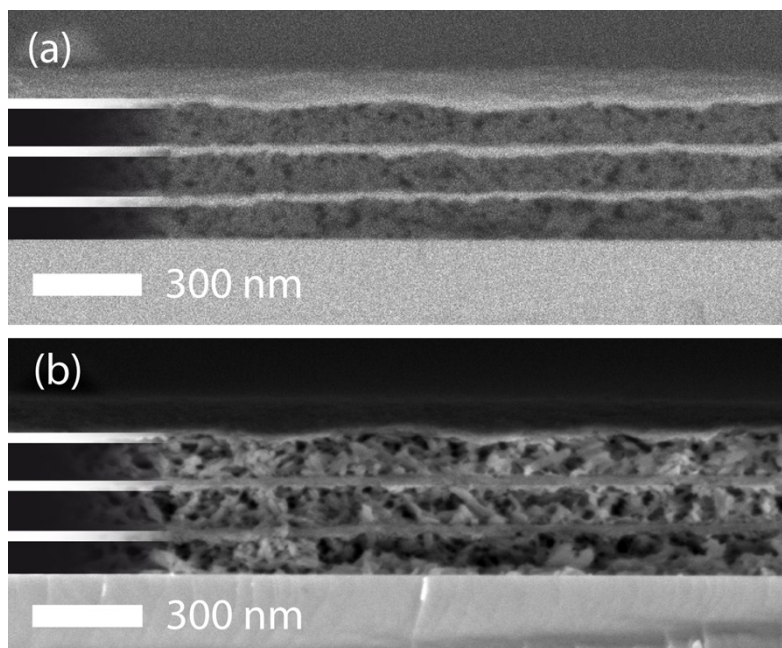


Figure S8: Cross-sectional SEM images of CAU-1-SBU on a silicon substrate acquired with a (a) back-scattered electron detector and (b) In-Lense detector with MOF layers of 117 ± 9 nm and TiO_2 layers of 30 ± 6 nm. The MOF layers are highlighted in black, the TiO_2 in white.

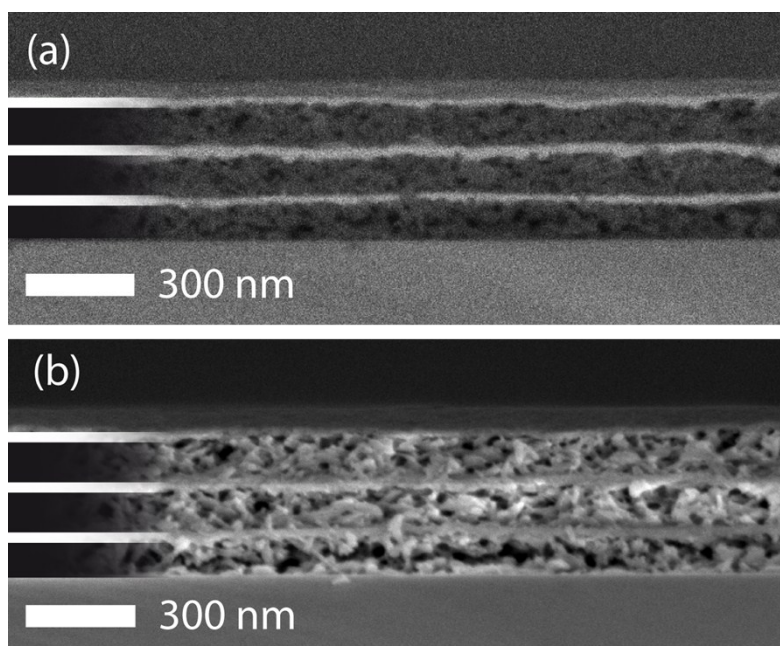


Figure S9: Cross-sectional SEM images of CAU-1-Hex on a silicon substrate acquired with a (a) back-scattered electron detector and (b) In-Lense detector with MOF layers of 112 ± 8 nm and TiO_2 layers of 30 ± 7 nm. The MOF layers are highlighted in black, the TiO_2 in white.

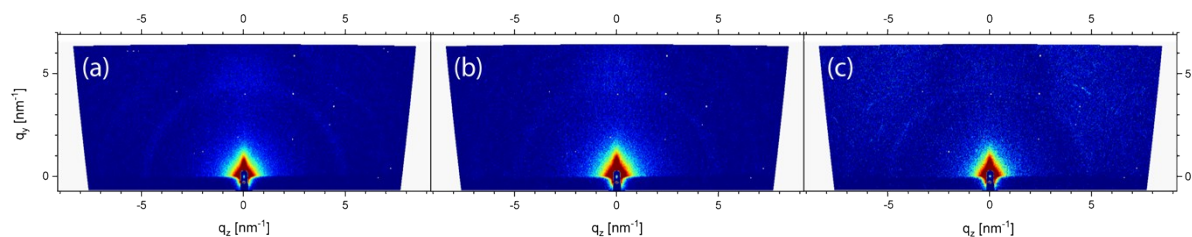


Figure S10: GISAXS measurements of the BSs (a) CAU-1-SBU, (b) CAU-1 and (c) CAU-1-Hex. Note the semicircle at 4.9 nm^{-1} corresponding to the 2θ reflection at 6.9° of the MOF.

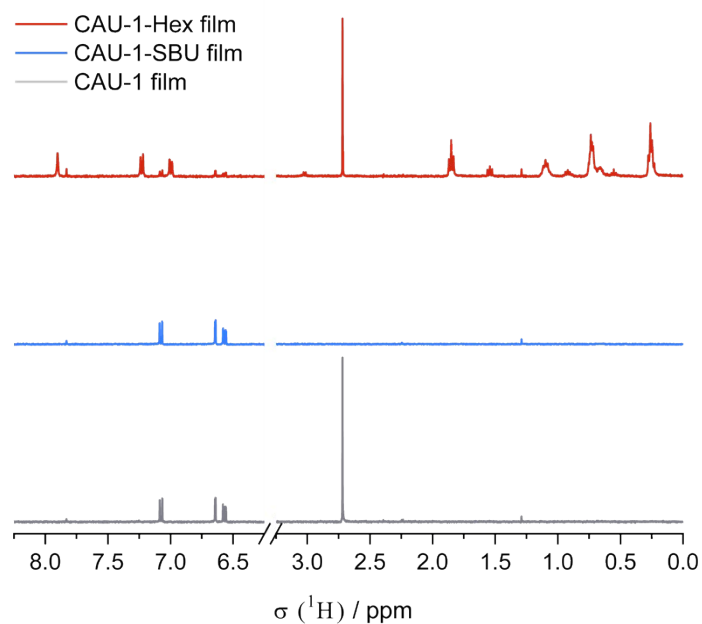


Figure S11: ^1H -NMR spectra of the directly dissolved CAU-1 (grey), CAU-1-SBU (blue) and CAU-1-Hex (red) films. Each spectrum is normalized to the sum of aromatic H signals (methylated and unmethylated). All samples were referenced to the ^1H signal of 2H of the unmodified linker.^[2]

The degree of methoxylation was calculated as explained above. The methoxy H-atoms: aromatic H-atoms were determined to be 1.13 for CAU-1, 0.00 for CAU-1-SBU and 1.10 for CAU-1-Hex (1:33 calc.), yielding a methoxylation degree of 85%, 0% and 83%, respectively. The degree of amidification was determined by the ratio of the aromatic H-atoms of the modified linker (1.00) to the total amount of aromatic H-atoms (1.13) yielding a modification degree of 88%. All samples show 1% methylation.

Table S2 Refractive indices and polarities at 25°C of the investigated solvents.

	Methanol	Water	Ethanol	iso-Propanol	Heptane
n	1.327	1.333	1.361	1.378	1.389
E_T^+	0.762	1.000	0.654	0.546	0.012

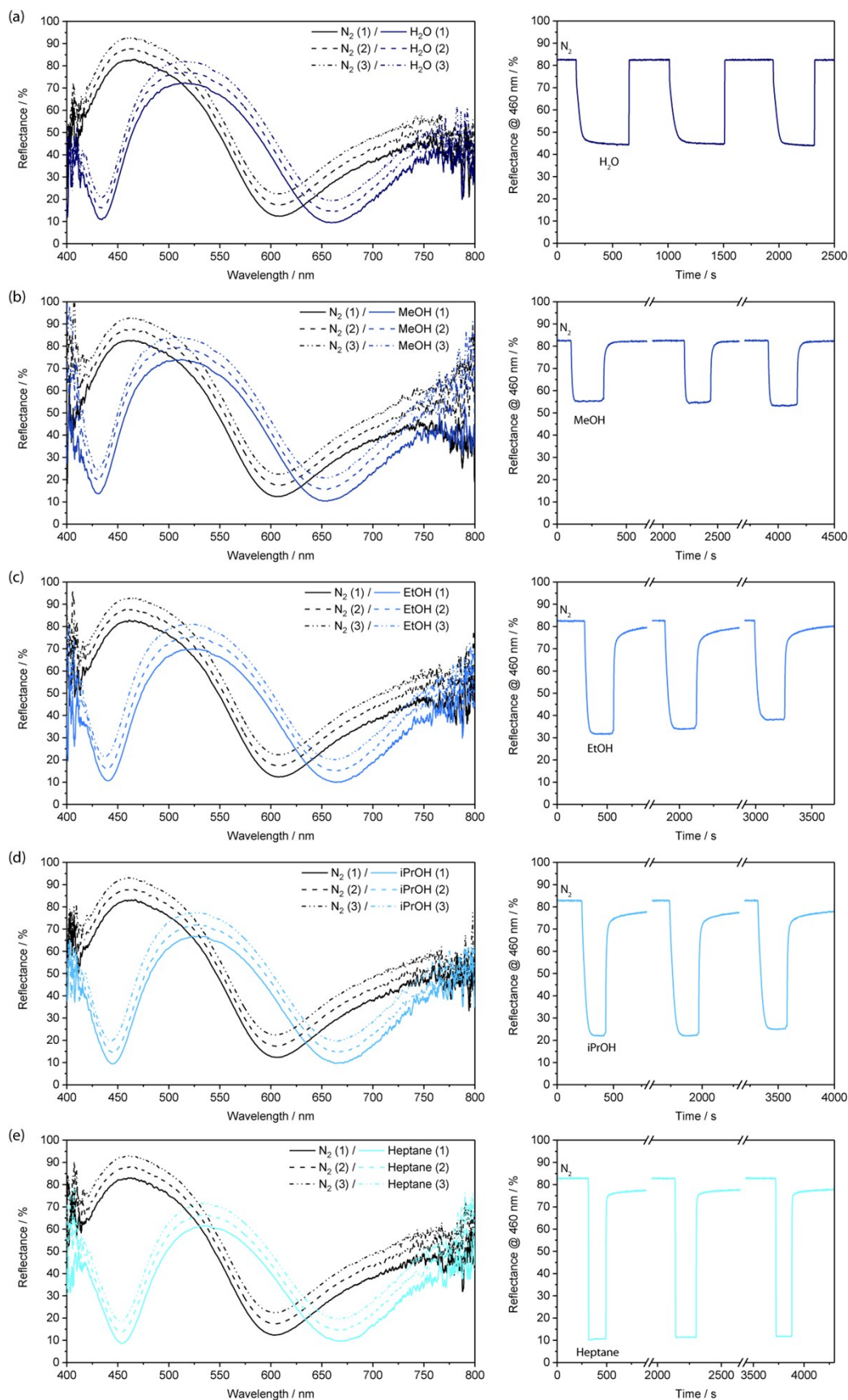


Figure S12: Reflectance spectra (left) and time-dependent reflectance at 460 nm (right) of the Bragg stack CAU-1-SBU exposed to alternating streams of nitrogen and (a) water, (b) methanol, (c) ethanol, (d) iso-propanol and (e) hexane vapor. The lined, dashed and dotted lines represent the first, second and third acquired spectra.

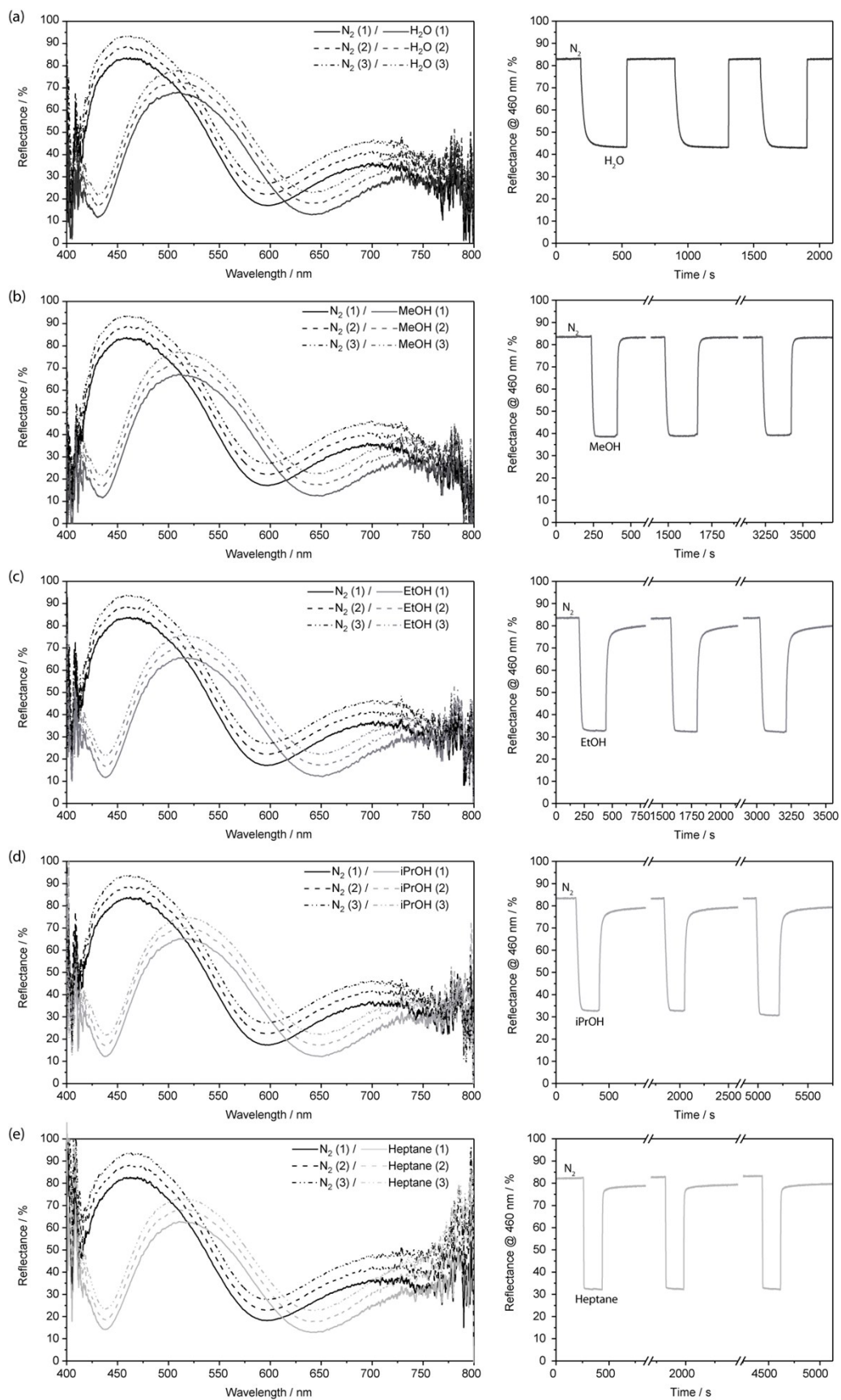


Figure S13: Reflectance spectra (left) and time-dependent reflectance at 460 nm (right) of the Bragg stack CAU-1 exposed to alternating streams of nitrogen and (a) water, (b) methanol, (c) ethanol, (d) iso-propanol and (e) hexane vapor. The lined, dashed and dotted lines represent the first, second and third acquired spectra.

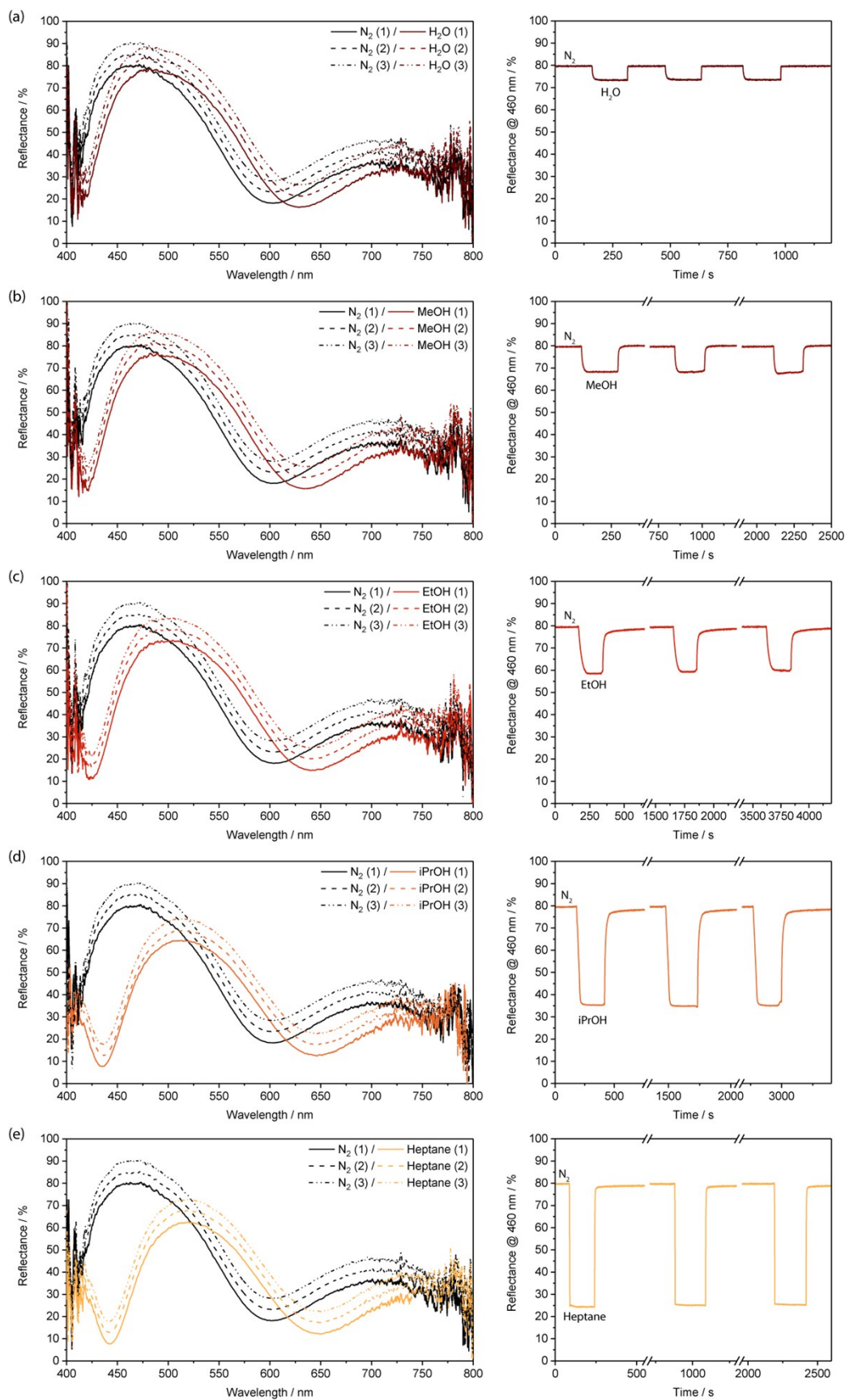


Figure S14: Reflectance spectra (left) and time-dependent reflectance at 460 nm (right) of the Bragg stack CAU-1-Hex exposed to alternating streams of nitrogen and (a) water, (b) methanol, (c) ethanol, (d) iso-propanol and (e) hexane vapor. The lined, dashed and dotted lines represent the first, second and third acquired spectra.

Table S3 Layer thicknesses and RIs obtained from spectroscopic ellipsometry

	CAU-1-SBU	CAU-1	CAU-1-Hex
d / nm	144	148	133
n_{eff}	1.388	1.362	1.350

Table S4 Modeled thicknesses and effective refractive indices of the constituent layers of the BSs. Note that the TiO_2 layer of CAU-1-SBU is also influenced by the thermal treatment as indicated by the higher RI in comparison to the other samples. Nonetheless, the discrimination capacity is still determined by the MOF layer.

	CAU-1-SBU		CAU-1		CAU-1-Hex	
	MOF	TiO_2	MOF	TiO_2	MOF	TiO_2
Thickness / nm	130	38	125	37	130	35
$n_{eff} (\text{N}_2)$	1.340	1.740	1.370	1.730	1.370	1.740
$n_{eff} (\text{H}_2\text{O})$	1.510	1.845	1.555	1.810	1.450	1.820
$n_{eff} (\text{MeOH})$	1.480	1.840	1.570	1.820	1.470	1.820
$n_{eff} (\text{EtOH})$	1.530	1.850	1.580	1.830	1.500	1.840
$n_{eff} (\text{iPrOH})$	1.560	1.850	1.580	1.820	1.555	1.820
$n_{eff} (\text{Heptane})$	1.595	1.830	1.580	1.790	1.590	1.800

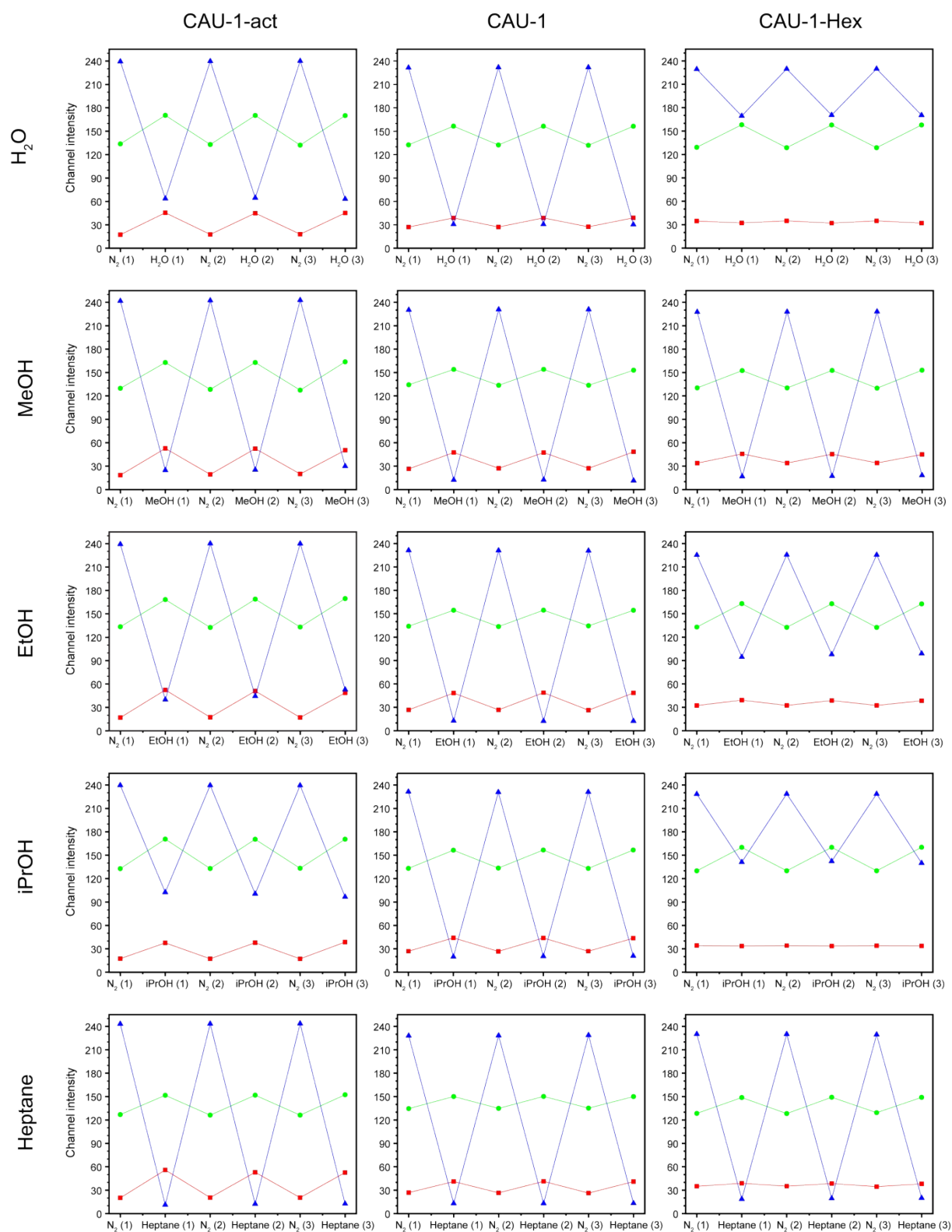


Figure S15 Intensity evolution of the R, G and B channel of photographic images for CAU-1-act, CAU-1 and CAU-1-Hex alternately exposed to nitrogen and the solvent vapors of water, methanol, ethanol, iso-propanol and heptane. The photographic images were acquired simultaneously to the reflectance spectra and processed to extract the mean values for the R, G and B channels.

Table S5 Intensities of the R channel and calculated ΔR values for CAU-1-act, CAU-1 and CAU-1-Hex extracted from the photographic images upon nitrogen and solvent vapor (water, methanol, ethanol, iso-propanol and heptane) exposure.

Red Channel										
		CAU-1-act			CAU-1			CAU-1-Hex		
Sorptive	No.	N2	Sorptive	Δ	N2	Sorptive	Δ	N2	Sorptive	Δ
H ₂ O	1	17.29	45.43	27.56	27.12	38.81	11.59	34.62	32.19	-2.78
	2	17.65	44.97		27.2	38.79		34.9	31.94	
	3	17.96	45.17		27.41	38.89		34.91	31.97	
	σ	0.33	0.23	0.50	0.15	0.05	0.10	0.16	0.14	0.30
MeOH	1	18.49	52.73	32.63	26.49	47.49	20.74	33.84	45.68	11.36
	2	19.35	52.47		27.19	47.3		34.01	45.38	
	3	19.89	50.40		27.19	48.32		34.06	44.94	
	σ	0.70	1.28	1.91	0.40	0.54	0.55	0.11	0.37	0.48
EtOH	1	16.94	52.43	33.59	26.73	48.41	21.99	32.31	39.25	6.43
	2	17.39	51.09		26.75	48.83		32.44	38.78	
	3	17.1	48.69		26.31	48.53		32.48	38.47	
	σ	0.23	1.90	1.95	0.25	0.22	0.28	0.09	0.39	0.48
iPrOH	1	17.42	37.62	20.75	26.87	44.11	17.03	34.2	33.55	-0.52
	2	17.26	37.83		26.7	43.87		34.13	33.58	
	3	17.16	38.63		26.87	43.56		34.08	33.74	
	σ	0.13	0.54	0.65	0.10	0.27	0.3	0.59	0.10	0.16
Heptane	1	20.11	55.89	33.47	26.81	41.13	14.64	34.98	38.91	3.64
	2	20.48	52.96		26.56	41.34		35.16	38.55	
	3	20.45	52.6		26.27	41.07		34.53	38.12	
	σ	0.21	1.81	2.01	0.27	0.14	0.27	0.32	0.40	0.28

Table S6 Intensities of the G channel and calculated ΔG values for CAU-1-act, CAU-1 and CAU-1-Hex extracted from the photographic images upon nitrogen and solvent vapor (water, methanol, ethanol, iso-propanol and heptane) exposure.

Green Channel										
		CAU-1-act			CAU-1			CAU-1-Hex		
Sorptive	No.	N2	Sorptive	Δ	N2	Sorptive	Δ	N2	Sorptive	Δ
H ₂ O	1	133.67	170.39	37.31	132.45	156.48	24.18	129.15	158.11	29.1
	2	132.89	170.25		132.3	156.4		128.67	157.83	
	3	132.15	170.01		131.91	156.33		128.65	157.83	
	σ	0.76	0.19	0.57	0.28	0.08	0.12	0.28	0.16	0.12
MeOH	1	129.77	162.83	34.65	134.31	153.99	19.79	130.34	152.49	22.52
	2	128.4	162.89		133.65	154.05		130.24	152.65	
	3	127.37	163.75		133.66	152.94		129.96	152.96	
	σ	1.21	0.51	1.66	0.38	0.63	0.57	0.19	0.24	0.43
EtOH	1	133.45	168.3	35.90	133.96	154.5	20.52	132.95	162.98	30.18
	2	132.47	168.84		133.55	154.56		132.54	162.86	
	3	133.04	169.54		134.39	154.42		132.47	162.67	
	σ	0.49	0.62	0.91	0.42	0.07	0.49	0.26	0.16	0.14
iPrOH	1	132.77	170.67	37.59	133.1	156.41	23.37	129.94	160.06	30.12
	2	132.91	170.45		133.5	156.69		130.02	160.12	
	3	133.19	170.52		133.06	156.67		130.02	160.17	
	σ	0.22	0.11	0.29	0.24	0.16	0.22	0.05	0.05	0.02
Heptane	1	126.92	151.7	25.49	134.54	150.09	15.27	128.45	148.81	20.29
	2	126.21	151.8		134.86	150.25		128.2	149.12	
	3	126.2	152.3		135.16	150.03		129.38	148.99	
	σ	0.41	0.32	0.67	0.31	0.12	0.36	0.62	0.15	0.66

Table S7 Intensities of the B channel and calculated ΔB values for CAU-1-act, CAU-1 and CAU-1-Hex extracted from the photographic images upon nitrogen and solvent vapor (water, methanol, ethanol, iso-propanol and heptane) exposure.

		Blue Channel								
		CAU-1-act			CAU-1			CAU-1-Hex		
Sorptive	No.	N2	Sorptive	Δ	N2	Sorptive	Δ	N2	Sorptive	Δ
H ₂ O	1	239.38	63.57	-175.95	231.4	30.69	-201.15	229.33	169.32	-59.55
	2	239.68	64.56		231.83	30.67		229.65	170.5	
	3	240.00	63.08		231.93	30.35		229.85	170.36	
	σ	0.31	0.75	0.91	0.39	0.40	0.78	0.26	0.65	0.44
MeOH	1	241.77	24.75	-215.74	230.27	12.26	-218.61	227.63	16.73	-210.49
	2	242.38	25.16		230.84	12.52		227.84	17.23	
	3	242.84	29.86		230.9	11.39		228.15	18.19	
	σ	0.54	2.84	2.39	0.34	0.59	0.79	0.26	0.74	0.48
EtOH	1	239.29	39.88	-194.08	231.37	12.73	-218.57	225.29	94.52	-128.3
	2	240.13	44.42		231.1	12.38		225.55	97.91	
	3	239.98	52.87		230.86	12.48		225.51	99.02	
	σ	0.45	6.59	6.31	0.25	0.18	0.18	0.14	2.35	2.22
iPrOH	1	239.72	102.48	-139.74	231.41	19.74	-210.77	228.4	141.16	-87.43
	2	239.64	100.55		230.81	20.43		228.63	142.28	
	3	239.48	96.58		231.12	20.85		228.6	139.89	
	σ	0.12	3.01	2.88	0.30	0.56	0.78	0.13	1.19	1.19
Heptane	1	243.13	11.19	-231.33	227.92	12.97	-215.25	230.11	18.55	-210.58
	2	243.31	12.36		228.26	13.05		230.05	19.44	
	3	243.63	12.53		228.7	13.12		229.48	19.91	
	σ	0.25	0.73	0.54	0.39	0.08	0.32	0.35	0.69	1.00

4. Supplemental References

- [1] A. Ranft, F. Niekief, I. Pavlichenko, N. Stock and B. V. Lotsch, *Chemistry of Materials*, 2015, **27**, 1961-1970.
 [2] T. Ahnfeldt, D. Gunzelmann, J. Wack, J. Senker and N. Stock, *CrystEngComm*, 2012, **14**, 4126-4136.